

## **Extreme Estimations of Non-Gaussian Wind Pressures Integrated with Hermite Polynomial Model and Bayesian Method**

\*Xing-Liang Ma<sup>1)</sup> and Fu-You Xu<sup>2)</sup>

<sup>1), 2)</sup> *School of Civil Engineering, Dalian University of Technology, Dalian, China*

<sup>1)</sup> *xingliangma@hotmail.com*

### **ABSTRACT**

The extreme value of wind pressure is very important for the design of cladding and glass curtain wall. For estimating the extreme values of non-Gaussian wind pressure processes, a novel approach integrated with the Hermite polynomial model and Bayesian method is proposed. The Hermite polynomial model is used to formulate the PDF of stationary non-Gaussian processes. Due to the randomness of aerodynamic effect and the incomplete ergodicity of collected data, the statistics of wind pressure samples always exhibit random properties, which violate the assumption of constants. In order to consider these intrinsic random properties, the parameters involved in Hermite polynomial model are estimated by Bayesian method, in which they are considered as random variables. Moreover, the empirical knowledge and the sampled information are integrated, and the final prediction of extreme wind pressure can be more reasonable. The efficacy of the newly-proposed approach is comprehensively demonstrated and verified by comparing its estimations with the directly observed data in long-duration wind tunnel tests.

### **1. INTRODUCTION**

Wind pressures on surface of buildings usually show nonGaussianity. A large amount of non-Gaussian wind pressure data were recorded from wind tunnel tests and in-situ measurements (Kasperski 2003; Holmes and Cochran 2003; Li and Hu 2015). Establishing a reasonable model for describing the parent non-Gaussian distribution is a key step for further estimation of the non-Gaussian extrema. Plenty of researches have been done to explore appropriate probabilistic models for non-Gaussian distribution (Masters and Gurley 2003; Gurley et al. 1997), and to propose accurate approaches to determine the extreme values of stationary non-Gaussian processes (Huang et al. 2014; Ding and Chen 2015).

Hermite polynomial model (HPM) is the most widely-applied transformation

---

<sup>1)</sup> Ph.D. student

<sup>2)</sup> Associate professor

formula between a non-Gaussian process and its underlying Gaussian pair (Winterstein 1985), it used the three-order Hermite polynomials to approximate the transformation relationship. Besides, HPM can also be used as probabilistic model for non-Gaussian distribution. Two shape parameters are required to be estimated to make the model work. The method of moment (MM) (Winterstein et al. 1994; Gurley et al. 1997; Yang et al. 2013) is a well-recognized approach to estimate the two shape parameters. Based on MM, several series of formulas for approximating the shape parameters were suggested (Winterstein 1988; Winterstein and Kashef 2000; Yang et al. 2013). Moreover, the HPM-based techniques for estimating the peak factor and extrema CDF of non-Gaussian processes were also discussed in many studies (Kareem and Zhao 1994; Kwon and Kareem 2011; Ding and Chen 2015).

Usually, the design wind pressure is determined on the basis of short-term (e.g., < 30 s) simultaneous pressure measurements on a scale model in a wind tunnel test. Due to the randomness of aerodynamic effect and the incomplete ergodicity of collected data, the statistics of the short-term wind pressure samples always exhibit random properties. In other words, the basic assumption of MM that the statistics are constants is not strictly valid. For parameter estimations, the Bayesian method can help provide more accurate resolutions. The parameters are regarded as random variables in Bayesian method, which is in accordance with the actual situation reflected by sampled data. Besides, the empirical knowledge of researchers and the sampled information are integrated in Bayesian method, by which the further prediction of wind pressure extrema can be more reasonable.

In this study, a ramification of Bayesian method which is integrated the features of MM and the method of maximum likelihood is proposed. The parent non-Gaussian distributions are respectively fitted by two HPMs those obtained from the novel method and from conventional method, and the extrema distribution is also further estimated. The fitting goodness is verified by comparing with the long-duration pressure records measured on a rigid model surface in a wind tunnel test, by which the applicability and accuracy of the newly-proposed method will be comprehensively validated.

## 2. HERMITE POLYNOMIAL MODEL

The HPM is a widely-applied method for bidirectional transformation between a standardized Gaussian variable and a standardized non-Gaussian variable. This method is based on the expansion of the non-Gaussian variable in terms of Hermite polynomials involving a standard Gaussian process (Winterstein 1985). This transformation is valid for a non-Gaussian process  $x(t)$  that can be expressed in terms of a standard Gaussian process  $u(t)$  through a monotonic function. For a softening process, whose skewness ( $\gamma_3$ ) and kurtosis ( $\gamma_4$ ) meets  $\gamma_4 \geq 3 + (1.25\gamma_3)^2$  (Winterstein and MacKenzie 2011), the HPM is briefly introduced here

$$x = \kappa \left[ u + h_3(u^2 - 1) + h_4(u^3 - 2u) \right], \quad (1a)$$

$$u = \left[ \sqrt{\xi^2(x) + c} + \xi(x) \right]^{1/3} - \left[ \sqrt{\xi^2(x) + c} - \xi(x) \right]^{1/3} - a, \quad (1b)$$

$$\xi(x) = 1.5b \left( a + \frac{x}{\kappa} \right) - a^3, \quad a = \frac{h_3}{3h_4}, \quad b = \frac{1}{3h_4}, \quad c = (b - 1 - a^2)^3, \quad (1c)$$

$$\kappa = (1 + 2h_3^2 + 6h_4^2)^{-1/2}, \quad (1d)$$

where  $h_3$  and  $h_4$  are two shape parameters. Based on HPM, the PDF of a standardized process  $x(t)$  can be expressed as (Grigoriu 1984)

$$f(x) = \frac{1}{\sqrt{2\pi}} \exp\left(-\frac{u^2}{2}\right) \frac{du}{dx}, \quad (2)$$

Assume Eq. (1b) is differentiable, the derivative  $du/dx$  is analytically derived as

$$\frac{du}{dx} = \frac{b}{2\kappa\sqrt{\xi(x)+c}} \left\{ \left[ \sqrt{\xi^2(x)+c} + \xi(x) \right]^{1/3} + \left[ \sqrt{\xi^2(x)+c} - \xi(x) \right]^{1/3} \right\}, \quad (3)$$

It is obvious that the PDF of  $x(t)$ , i.e., Eqs. (2), only depends on  $h_3$  and  $h_4$ , which can be seen as the shape parameters of the non-Gaussian distribution. For determining  $h_3$  and  $h_4$ , the MM was often utilized. In addition, on the basis of optimal results that minimize the fit errors for skewness and kurtosis of the HPM, Winterstein et al. (1994) proposed simple expressions for shape parameters  $h_3$  and  $h_4$ . These expressions are intended for application in the ranges of  $0 < \gamma_4 < 15$ ;  $1.5\gamma_3^2 + 3 < \gamma_4$ , which may include most cases of practical interests (Winterstein and Kashef 2000).

$$h_3 = \frac{\gamma_3}{6} \left[ \frac{1 - 0.015|\gamma_3| + 0.3\gamma_3^2}{1 + 0.2(\gamma_4 - 3)} \right], \quad (4a)$$

$$h_{40} = \frac{\left[ 1 + 1.25(\gamma_4 - 3) \right]^{1/3} - 1}{10}, \quad (4b)$$

$$h_4 = h_{40} \left[ 1 - \frac{1.43\gamma_3^2}{\gamma_4 - 3} \right]^{1 - 0.1\gamma_4^{0.8}}, \quad (4c)$$

It is noted that the MM has its specific strengths and weaknesses. MM endows the data in the tail area with more weights compared with the data in bulk. Therefore, the estimated PDF by the MM fits the tails relatively better than the bulk. However, only the third- and fourth-moment may be insufficient to capture the probabilistic feature of tail areas, and usually results in an overestimation of the extrema (Ishikawa 2004). A Bayesian method combined the features of the MM and the method of maximum likelihood will be discussed in next section to solve this challenging issue.

### 3. BAYESIAN METHOD for PARAMETERS ESTIMATION of HPM

#### 3.1 Fundamental idea

According to Bayesian theory, the distribution parameters are supposed as random variables, rather than constants. The parameters are distributed as another PDFs (prior distributions). If some data are sampled, a conditional PDF can be identified based on the prior experience and the new sampled information. The posterior PDF can be further expressed in a Bayesian manner as:

$$\pi(\theta|x) = \frac{f(x|\theta)\pi(\theta)}{\int f(x|\theta)\pi(\theta)d\theta} \propto f(x|\theta)\pi(\theta), (5)$$

where  $\pi(\theta)$  and  $\pi(\theta|x)$  are the prior and posterior distributions of the model parameters;  $f(x|\theta)$  is the likelihood function (conditional probability); the symbol  $\propto$  means be proportional to;  $\theta$  is a continuous parameter vector and  $x$  is sample data.

#### 3.3 Prior distribution

According to the study of Yang and Tian (2015), the shape parameters  $h_3$  and  $h_4$  in HPM are approximately distributed as Gaussian type, when the HPM is used to describe the probability distribution of long-duration wind pressure. For computational simplicity, the prior joint PDF of  $h_3$  and  $h_4$  is assumed as a 2-dimensional Gaussian PDF. And this approximation error would be remedied by the sampling information. Specifically, the covariance matrix of  $h_3$  and  $h_4$  is assumed as  $\begin{bmatrix} 0.02^2, 0.8 \times 0.02 \times 0.005; 0.8 \times 0.02 \times 0.005, 0.005^2 \end{bmatrix}$  for positive  $\gamma_3$ , and  $\begin{bmatrix} 0.02^2, -0.8 \times 0.02 \times 0.005; -0.8 \times 0.02 \times 0.005, 0.005^2 \end{bmatrix}$  for a negative  $\gamma_3$ . The expected value of  $h_3$  and  $h_4$  are obtained based on the MM by substituting  $\gamma_3$  and  $\gamma_4$  of sampled data into Eq. (4). Therefore, the prior PDF of shape parameters is related to the estimations of MM. In other words, it united the empirical and the analytical elements.

#### 3.4 Posterior distribution

The conditional probability  $f(x|\theta)$  of the sampled data can be calculated as

$$f(x|\theta) = \prod_{i=1..n} f(x_i), (6)$$

where  $f(x_i)$  is formulated by Eq. (2);  $x_i$  is the  $i^{th}$  data of all  $n$  samples. Namely,  $f(x|\theta)$  is the likelihood function of sampled data, which endows the Bayesian estimation with the property of the method of maximum likelihood. After the posterior distribution  $\pi(\theta|x)$  is determined, the expected value of  $\pi(\theta|x)$  can be calculated as the final result of Bayesian estimation. Although it is difficult to calculate the

denominator and the analytical expression of numerator in Eq. (5), the Metropolis-Hastings sampling method (MHSM) (Metropolis et al. 1953) can be used to solve the issue.

### 3.5 Implementation of the MHSM

The MH sampling method is based on the Markov chain Monte Carlo (MCMC) methodology, which is a general computational approach that replaces the analytical integration of complex or high-dimensional distributions. The goal of MCMC is to design a Markov chain such that the stationary distribution of the chain is exactly the distribution that is desired to sample from (Metropolis et al. 1953). The MHSM is one of the algorithms that developed from the MCMC, based on which samples can be generated from the complicated posterior joint PDF, e.g., Eq. (5). Two essences are included in the MHSM, one is to generate a candidate point  $\theta^*$  by using a proposal distribution  $q(\theta|\theta^{t-1})$ . Another one is to either accept the proposal as  $\theta^t$  or reject it. For sampling from Eq. (5), the specific sampling procedure is listed as follows:

- a) Set  $t = 1$ ;
- b) Calculate the initial value of  $H = (h_3, h_4)$  by Eq. (4), and set  $\theta^0 = H$ ;
- c) Repeat
  - $t = t + 1$
  - Generate a proposal  $\theta^*$  from  $q(\theta|\theta^{t-1})$ ;
  - Evaluate the acceptance probability  $\alpha = \min\left(1, \frac{f(\theta^*|x) q(\theta^{t-1}|\theta^*)}{f(\theta^{t-1}|x) q(\theta^*|\theta^{t-1})}\right)$ ;
  - Generate a  $\beta$  from a Uniform(0,1) distribution;
  - If  $\beta < \alpha$ , accept the proposal and set  $\theta^t = \theta^*$ , else set  $\theta^t = \theta^{t-1}$ ;
- d) Until  $t$  attains the desired number of samples.

The average of the samples of  $h_3$  and  $h_4$  can be considered as the final results of Bayesian estimation. More details of the MH sampling can be referred to Hastings (1970).

Once the shape parameters  $h_3$  and  $h_4$  are determined, the non-Gaussian wind pressure records can be modeled by HPM. Then the probability distribution of extreme wind pressure and the peak factor can be easily obtained as recommended by Kwon and Kareem (2011).

#### 4. DATA RESOURCE

Wind pressures on the surfaces of the rigid model of a tall building were measured for a long time in the boundary layer wind tunnel at Dalian University of Technology, China. The working section of the wind tunnel laboratory is 3 m in width, 2.5 m in height, and 18 m in length. Spires and roughness cube elements were used to generate the desired boundary layer wind profile. A boundary layer corresponding to the urban terrain (Category C) in Chinese code GB50009-2012 (National Standard of the People's Republic of China, 2012) was simulated.

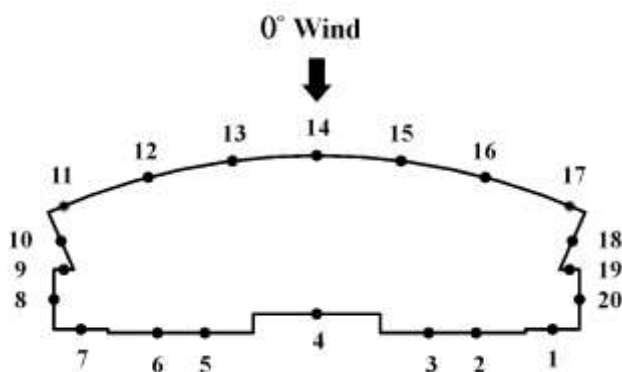


Fig. 1 Arrangement of pressure taps and wind directions



Fig. 2 A picture of the wind tunnel test

The tests were conducted on a 54 cm high rigid model with a length scale of 1: 200. The velocity scale was set as 1: 4, and the corresponding time scale was 1: 50. The plane layout of Taps 1-20 and a picture of the test are respectively shown in Fig. 1 and Fig. 2. The sixty taps on the three layers, i.e., at the height of 23, 35, and 46cm, were numbered as 1-20, 21-40, and 41-60, respectively. At a sampling frequency of 312.5 Hz, a long time history of 20 min was recorded in  $0^\circ$  wind direction as shown in Fig. 1. Correspondingly, the time duration for full-scale measurement was 1000 min, i.e., 100 repeats of 10-min standard time intervals.

#### 5. COMPARISON of FITTING GOODNESS for NON-GAUSSIAN DISTRIBUTION

In this section, the Bayesian-based HPM and the MM-based HPM will be applied to model the wind pressure records, and their fitting performance will be compared. Two taps, i.e., No. 1 and No. 7 are taken as the computational examples. The long-duration time histories are divided into 100 segments with 10-min standard time intervals. The skewness and kurtosis of the total 200 segments of two taps are dotted in Fig. 3.

Due to the randomness of aerodynamic effect and the incomplete ergodicity of collected data, the statistics of short segments exhibit random properties as shown in Fig. 3, which violates the assumption of constants. However, for the MM, e.g., in Eq. (4),

the  $\gamma_3$  and  $\gamma_4$  are considered as the constants which are equal to the skewness and kurtosis of the samples. Substitute these  $\gamma_3$  and  $\gamma_4$  into Eq. (4), the calculation results of  $h_3$  and  $h_4$  are dotted in Fig. 4. It is obvious that the shape parameters of HPM also show the random characteristics.

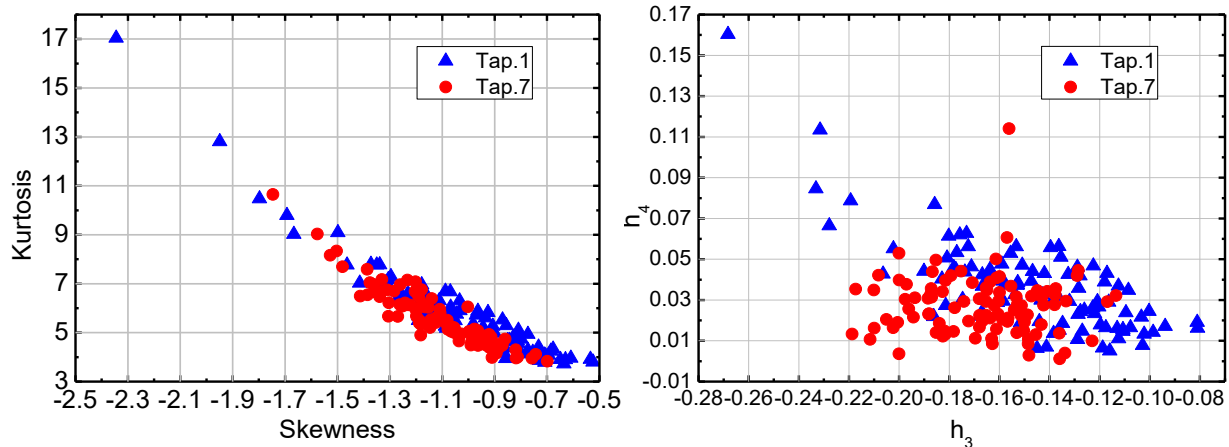


Fig. 3 Skewness and kurtosis of wind pressures    Fig. 4  $h_3$  and  $h_4$  for two taps

The variance of the statistical moments becomes lower when the length of the segments increases. Only if the length of segments were assigned long enough, the statistical moments could be approximated as constants. Nevertheless, the wind tunnel tests and field measurements are always kept for a quite short time, e.g., less than 1min for wind tunnel tests, which probably leads to the skewness and kurtosis of the sample deviate farther away from their expected values. It also affect the estimation accuracy of the shape parameters  $h_3$  and  $h_4$ . In Bayesian method,  $h_3$  and  $h_4$  are considered as variables, and the probable errors caused by the randomness of sampled data can be theoretically reduced. The following discussion is conducted on the basis of the assumption that only the first 1min, i.e., the five segments are in hand. The standardized time histories of the first five segments at the two taps are plotted in Fig. 5, and their skewness and kurtosis are also listed.

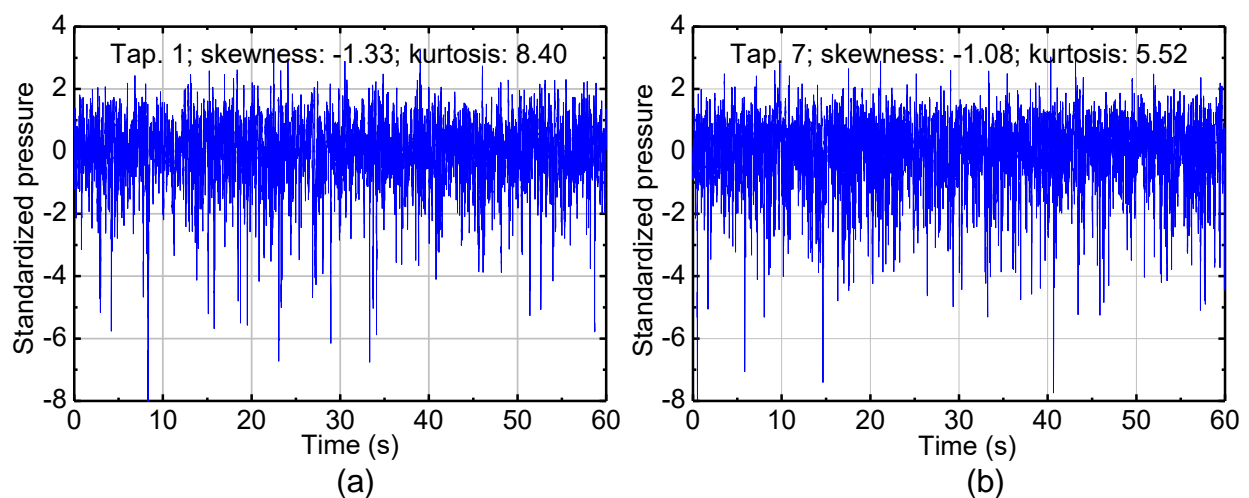


Fig. 5 Time histories of wind pressure at two taps: (a) Tap 1; (b) Tap 7

Two sets of shape parameters in HPM are respectively calculated by Eq. (4) and the proposed Bayesian method. The corresponding PDF curves are plotted in Fig. 6. The real target of the utilization of HPM is to predict the long-term probabilistic characteristics by using the short-term sampled data in hand. Therefore, the histograms of the total 100 segments are also shown in Fig. 6 as the benchmark reference for assessing the fitting goodness. The skewness and kurtosis of the entire sampled data is -1.08 and 6.16 for Tap 1, -1.14 and 5.80 for Tap 7, respectively. The third- and fourth- moments of the short-term data for Tap 7 are very close to the statistics of the entire data. However, the corresponding pairs deviates far from each other for Tap 1. Therefore, the MM-based HPM fits the histogram of Tap. 7 quite well in the bulk, due to the statistics of short-term data for Tap. 7 in hand is close to the long-term data coincidentally. But it lose accuracy for Tap. 1, because of the big difference between the statistics of short-term data in hand and the long-term data. By comparison, the Bayesian-based HPM offered both taps outstanding fit in the mean region. For further exploring the fitting performance of two methods for the tails area, the semi-log scales comparisons of PDF are shown in Fig. 7.

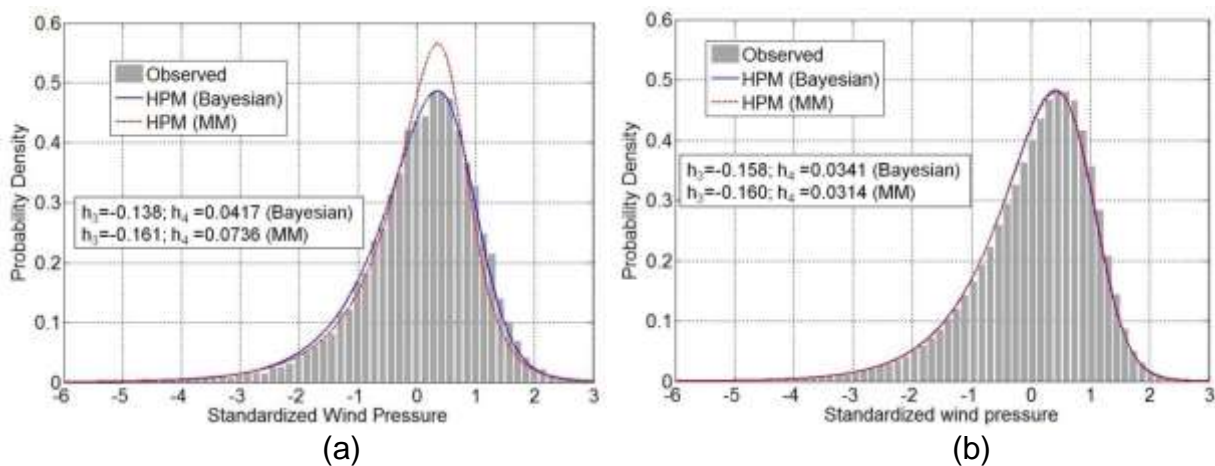


Fig. 6 Comparisons of fitted PDFs (a) Tap 1; (b) Tap 7

The comparative results in tail areas are similar to those in the mean region. The Bayesian-based HPM did much better than the MM-based HPM for Tap 1 on both long-tail and short-tail side.

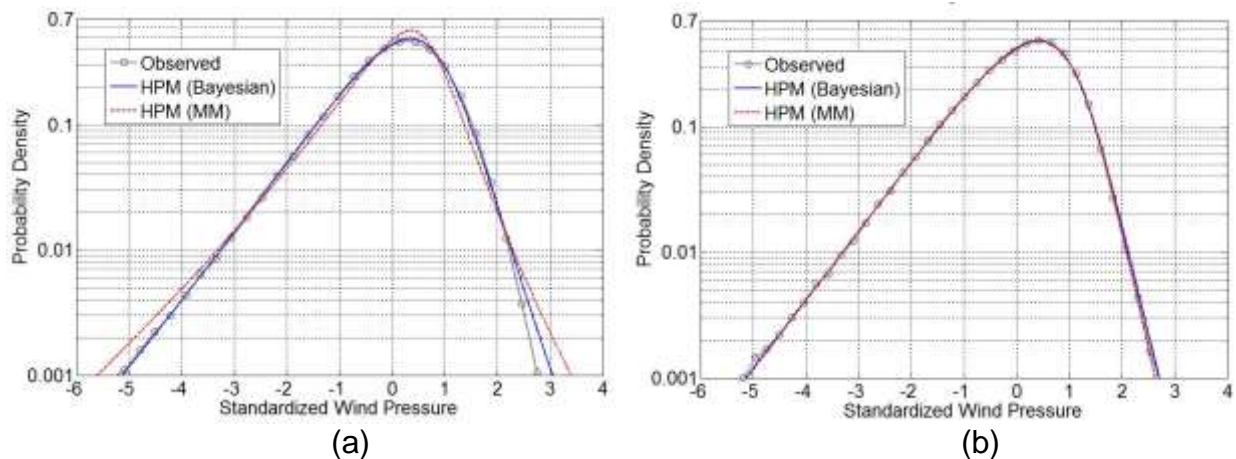


Fig. 7 Comparisons of fitted PDFs in semi-log scale (a) Tap. 1; (b) Tap. 7

## 6. Estimation of Wind Pressure Extrema

After the parent non-Gaussian distribution is fitted by the HPM, the CDF of the non-Gaussian extrema can be estimated (Kwon and Kareem 2011). Due to the extrema on the long-tail side of the non-Gaussian distribution are relatively larger than those on the short-tail side, the extrema on long-tail side is usually of more interest for structure design. Accordingly, the estimated CDFs of extrema on the long-tail side from two methods are plotted in Fig. 8. The empirical CDF of the minimum values from 100 segments are also plotted in Fig. 8 as the standard value for comparison. Meanwhile, the lower and the upper confidence bounds (LCB and UCB) at the confidence level of 95% are also calculated and marked. For Tap. 7, both methods matches the empirical CDF well. The derived extrema CDFs is located between the LCB and the UCB. The good performance is beneficial from the high-level fitting of the parent distribution as shown in Fig. 7b. However, there is an obvious gap between the matching goodness of two methods for Tap 1. The estimation from MM-based HPM lost its accuracy, but the estimation from Bayesian-based HPM still matches the empirical CDF outstandingly, by which the accuracy of the Bayesian-based method is convincingly demonstrated.

A further discussion is conducted by integrating the Fig. 7 and 8. The accurate estimation of the probabilistic properties of the extrema requires accurate fitting of the parent distribution. However, if the sampled data in hand is not long enough, their statistics cannot be regarded as constants. Once they are considered as constants, for instance in the method of moment and the method of maximum likelihood, the fitting accuracy of parent distribution cannot be guaranteed.

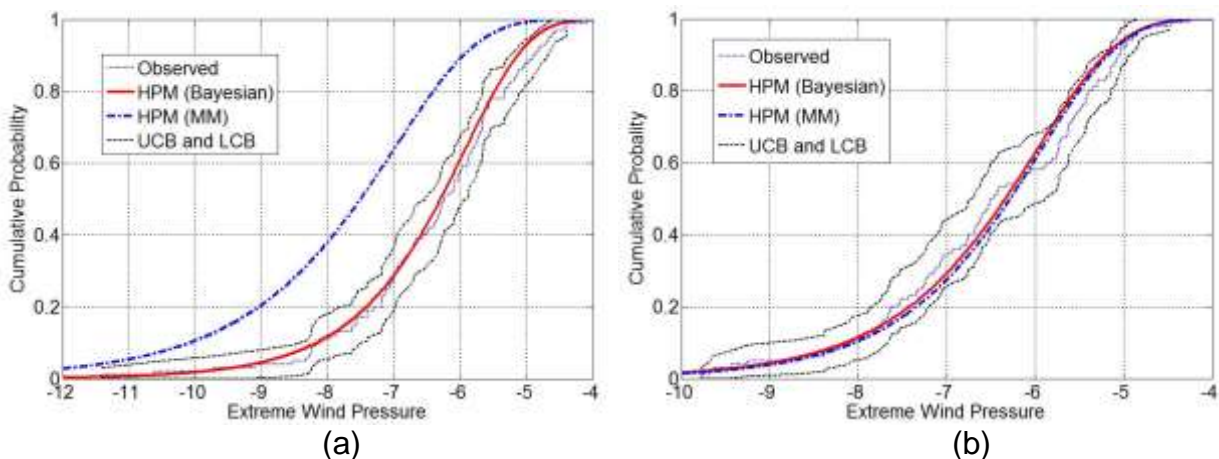


Fig. 8 Comparisons of extrema CDF on the long-tail side: (a) Tap 1; (b) Tap 7

## 7. Concluding Remarks

In this study, a Bayesian-based method is proposed to calculate the shape parameters of the Hermite polynomial model (HPM). Based on the long-duration wind pressure records on the surfaces of a high-rise building model in wind tunnel tests, the parent non-Gaussian distributions at two Taps were fitted by the Bayesian method and the conventional method (method of moment). The fitting goodness of the two methods is comprehensively compared and analyzed. Compared with conventional method, the Bayesian-based method has a better fitting performance of non-Gaussian distribution in both bulk and tail regions. The estimation accuracy of the extrema CDF by the new method is also fully verified by comparing with the conventional method and the directly observed results.

## Acknowledgement

The research is jointly supported by the National Program on Key Basic Research Project (973 Program, 2015CB057705) and National Science Foundation of China (51478087).

## REFERENCES

- Ding, J., and Chen, X. Z. (2015). "Moment-Based translation model for hardening non-Gaussian response processes." *J. Eng. Mech.*, ASCE, 06015006.
- Huang, M. F., Lou, W., Pan, X., Chan, C. M., and Li, Q. S. (2014). "Hermite Extreme Value Estimation of Non-Gaussian Wind Load Process on a Long-Span Roof Structure." *Journal of Structural Engineering*, ASCE, 140(9): 04014061.
- GB 50009-2012. (2012). *Load code for the design of building structures*, Architecture Industrial Press of China, Beijing (in Chinese).
- Grigoriu, M. (1984). "Crossings of non-Gaussian translation processes." *J. Eng. Mech.*, ASCE, 110(4): 610-620.
- Gurley, K. R., Tognarelli, M. A., and Kareem, A. (1997). "Analysis and simulation tools for wind engineering." *Probabilistic Engineering Mechanics*, 12(1): 9-31.

- Hastings, W. K. (1970). "Monte Carlo sampling methods using Markov chains and their applications." *Biometrika*, 57(1):97-109.
- Holmes, J. D., and Cochran, L. S. (2003). "Probability distributions of extreme pressure coefficients." *J. Wind Eng. Ind. Aerodyn.*, 91(7): 893-901.
- Huang, M. F., Lou, W., Pan, X., Chan, C. M., and Li, Q. S. (2014). "Hermite Extreme Value Estimation of Non-Gaussian Wind Load Process on a Long-Span Roof Structure." *J. Struct. Eng., ASCE*, 140(9): 04014061.
- Ishikawa, T. (2004). "A study on wind load estimation method considering dynamic effect for overhead transmission lines." PhD thesis, Waseda University.
- Kasperski, M. (2003). "Specification of the design wind load based on wind tunnel experiments." *Journal of Wind Engineering and Industrial Aerodynamics*, 91(4): 527-541.
- Kwon, D. K., and Kareem, A. (2011). "Peak factors for non-Gaussian load effects revisited." *J. Struct. Eng., ASCE*, 137(12): 1611-1619.
- Li, Q. S., and Hu, S. Y. (2015) "Monitoring of wind effects on an instrumented low-rise building during severe tropical storm." *Wind and Structures*, 20(3):469-488.
- Masters, F., and Gurley, K. R. (2003). "Non-Gaussian simulation: Cumulative distribution function map-based spectral correction." *J. Eng. Mech., ASCE*, 129(12):1418-1428.
- Metropolis, N., Rosenbluth, A. W., Rosenbluth, M. N., Teller, A., and Teller, A. H. (1953). "Equation of state calculations by fast computing machines." *J. Chem. Phys.*, 21(6), 1087-1092.
- Tognarelli, M. A., Zhao, J., and Kareem, A. (1997). "Equivalent statistical cubicization for system and forcing nonlinearities." *J. Eng. Mech.*, 123(8), 890-893.
- Winterstein, S. R. (1985). "Non-normal responses and fatigue damage." *J. Eng. Mech.*, 111(10), 1291-1295.
- Winterstein, S. R. (1988). "Nonlinear Vibration Models for Extremes and Fatigue." *J. Eng. Mech., ASCE*, 114(10): 1772-1790.
- Winterstein, S. R., Ude, T. C., and Kleiven, G. (1994). "Springing and slow-drift responses: predicted extremes and fatigue vs. simulation." *Proceedings, Behaviour of Offshore Structures at Sea -- BOSS-94*, 3:1-15.
- Winterstein, S. R., and Kashef, T. (2000). "Moment-based load and response models with wind engineering applications." *J. Sol. Energy Eng.*, 122, 122-128.
- Winterstein, S. R., and Mackenzie, C. A. (2011) "Extremes of Nonlinear Vibration: Models Based on Moments, L-Moments, and Maximum Entropy." *Journal of Offshore Mechanics and Arctic Engineering*, 135(2):185-195.
- Yang, L. P., Gurley, K. R., and Prevatt, D. O. (2013). "Probabilistic modeling of wind pressure on low-rise buildings." *J. Wind Eng. Ind. Aerodyn.*, 114: 18-26.
- Yang, Q. S., and Tian, Y. J. (2015). "A model of probability density function of non-Gaussian wind pressure with multiple samples." *Journal of Wind Engineering and Industrial Aerodynamics*, 140:67-78.